2011 50th IEEE Conference on Decision and Control and
European Control Conference (CDC-ECC)
Orlando, FL, USA, December 12-15, 2011

H^∞ current control strategy for the neutral point of a three-phase inverter

Tomas Hornik and Qing-Chang Zhong

***Abstract*— In this paper, an H^∞ current controller is proposed to maintain a balanced neutral point for a three-phase four-wire inverter, which can be used in microgrid applications. The neutral-point circuit consists of a conventional neutral leg and a split DC link. The neutral point is balanced with respect to the two DC source terminals (as required, e.g., in neutral-point-clamped three-level converters) even when the neutral current is large so that the inverter can be connected to an unbalanced load and/or utility grid. The controller, designed by using the H^∞ control techniques, can eliminate the current flowing through the split capacitors. This leads to very small deviations of the neutral point from the mid-point of the DC source, in spite of the possibly large neutral current. Experimental results are presented to demonstrate the excellent performance of the proposed control scheme.**

***Index Terms*— DC-AC power converter, multi-level PWM converter, DC-link balancing, neutral line, 3-phase 4-wire power system, H^∞ control**

I. Introduction

Rapidly increasing energy demand from the industrial and commercial sectors, especially in the current climate of increased concerns about environmental changes, has led to fast development of Distributed Power Generation Systems (DPGS) based on renewable energy sources. A more recent concept is to group DPGS and the associated loads to a common local area to form a small power system called a microgrid. The introduction of microgrids improves power quality, reduces transmission line congestion, decreases emission and energy losses, and effectively facilitates the utilisation of renewable energy resources [1], [2], [3], [4], [5], [6].

In some circumstances, the inverters used in microgrids and/or DPGS must supply a mixture of single- and three-phase loads via a four-wire three-phase distribution network. The neutral line is usually needed to provide a current path for possible unbalanced loads and the traditional six-switch inverter must be supplemented with a neutral connection. If the neutral point of a four-wire system is not well balanced, then the neutral-point voltage may deviate severely from the real midpoint of the DC source. This deviation of the neutral point may result in an unbalanced or variable output voltage, the presence of the DC component, larger neutral current or even more serious problems. Thus, the generation of a balanced neutral point in a simple and effective manner has become an important issue [7].

T. Hornik is with Department of Electrical and Electronic Engineering, The University of Liverpool, UK.

Q.-C. Zhong is with Loughborough Centre in Control Engineering, Department of Aeronautical and Automotive Engineering, Loughborough University, UK.

All correspondences should be addressed to Q.-C. Zhong, Tel: +44-1509-227 223, Fax: +44-1509-227 250, Email: zhongqc@ieee.org.

Three different circuit topologies have been widely used to generate a neutral point [7], [8]. The most popular topology is a split DC link, shown in Figure 1 (a), with the neutral point clamped at half of the DC link voltage. Since the neutral current flows through capacitors, high capacitance is necessary. Moreover, the neutral point usually shifts following capacitors and/or switches differences. To improve performance of the split DC link topology, different neutral point balancing strategies are reported, usually using redundant states of the Space Vector Pulse Width Modulation (SVPWM) [9], [10], [11] or varied voltage-balancing modulation techniques as proposed in [12], [13]. The main drawback is that the neutral point balancing is not fully decoupled from the three-phase converter control and, as a result, the power quality of the output voltages can be significantly affected. Figure 1 (b) shows another way to handle the neutral point control. An additional fourth leg, called the neutral leg, is added to a conventional three-leg converter. Various control strategies are available for this topology [14], however the additional neutral leg again cannot be fully independently controlled to maintain a stable neutral point. The third topology, an actively balanced split DC link topology shown in Figure 1 (c), is the combination of the first two (split DC link and the additional neutral leg). The control of the neutral point in this case can be decoupled from the control of the three-phase converter [15], [16], [7], [8].

In this paper, a current control strategy is proposed for the actively balanced split DC link topology. The controller is designed by using the H^∞ control techniques to eliminate the current i_C flowing through the split capacitors. Since the neutral point can slightly shift due to the mismatch of capacitors and/or the non-linearity of switches, an extra voltage control loop is added to bring the shift back to normal. The proposed strategy brings very small deviations of the neutral point from the mid-point of the DC source, in spite of the possibly large neutral current. Experimental results are presented to demonstrate the excellent performance of the proposed control scheme. In addition, the performance of the proposed H^∞ current controller is compared with proportional and H^∞ voltage-current controllers proposed in [8] and [7] respectively. Although it is not a focus of this paper, the proposed control strategy can be applied to maintain the mid-point of multi-level inverters.

The rest of the paper is organised as follows. The overall structure of the system is presented in Section II, followed by the H^∞ current controller designed in Section III and the voltage control loop designed in IV. The experimental setup is briefly described in Section V, followed with experimental

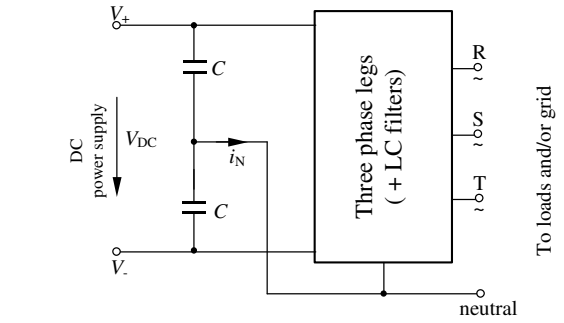

(a) the split DC link

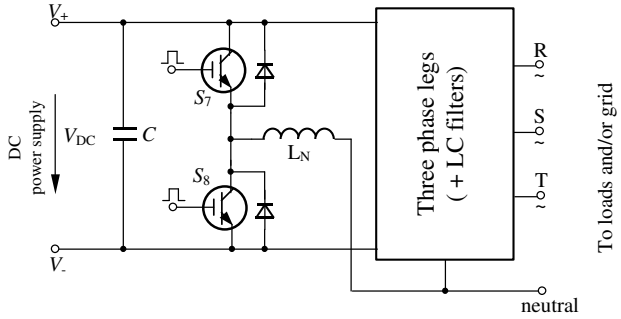

(b) additional neutral leg

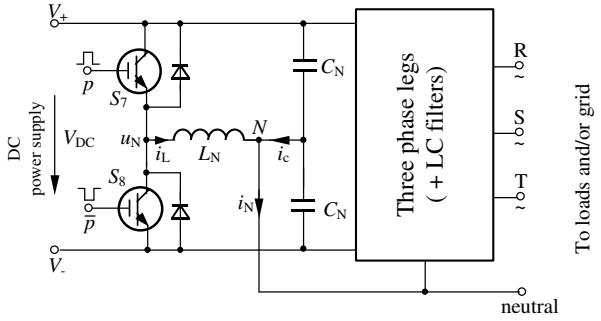

(c) the combination of (a) and (b): the actively balanced split DC link

Fig. 1. Circuit topologies to generate a neutral point [7], [8]

results. Finally, conclusions are made in Section VI.

II. Description of the System

As mentioned previously, the circuit topology shown in Figure 1 (c), is the combination of the split DC link and the neutral leg topologies [7], [8] and the control of the neutral point is decoupled from the control of the three-phase inverter. The total DC-link voltage is the difference between the two capacitor voltages measured with respect to the neutral point

$$V_{DC} = V_{CN+} - V_{CN-}.$$

Since the control objective is to maintain the point N as a neutral point, then the average voltage

$$V_{ave} = \frac{V_{CN+} + V_{CN-}}{2} \tag{1}$$

is expected to be very close to 0 all the time. As a result, i_L is expected to be almost equal to i_N. This means that the majority of the neutral current should flow through the inductor L_N but not through the capacitors C_N, i.e.,a smaller current i_C brings a smaller variation of the neutral point N. Hence, the capacitors are not necessarily very large, as those needed in the conventional split DC link. The control strategy will be developed to to make i_C as small as possible (ideally $i_C = 0$).

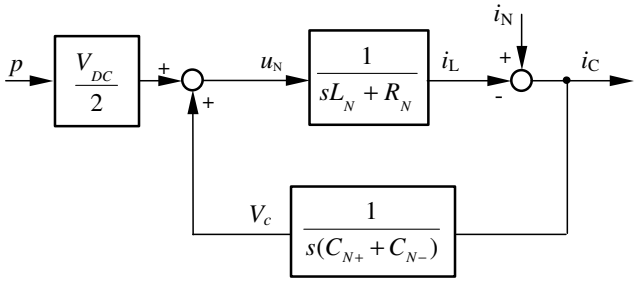

Fig. 2. The block diagram of the neutral leg

III. Design of an H^∞ Current Controller

A. Controller Description

The block diagram of the neutral leg is shown in Figure 2, where p is the duty cycle for the switches. The resistance of the inductor is included and the capacitors are assumed to be different. The control objective is to maintain a stable and balanced neutral point, i.e., to make i_C as small as possible while maintaining the stability of the system.

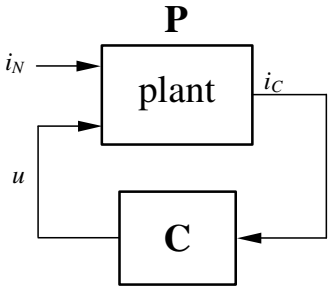

Fig. 3. The block diagram of the H^∞ control scheme

The sketch of the H^∞ current control scheme is shown in Figure 3, where P is the transfer function of the plant and C is the transfer function of the controller. The controller C is designed by solving a weighted sensitivity H^∞ problem [17], as formulated later, to assure the stability of the entire system, which implies that the current i_C will converge to a small value. The neutral current i_N is regarded as an external disturbance and the control action is $u = p$.

B. Formulation into a Standard H^∞ Problem

Since the current i_C contains significant ripples at the switching frequency, it is measured through a low-pass filter.

The remaining ripple after this filter can be interpreted as a measurement noise n. The disturbance is expected to be within a certain frequency range so a weighting function W is introduced to reflect this. In order to avoid a large control action, a weighting factor μ is introduced. A new variable I_n, which is proportional to the measurement noise n, is also introduced via a factor ζ. The weighting factors ζ and μ can be used to adjust the relative importance of the disturbances i_N and n in the H^∞ norm minimisation process. The H^∞ control problem, as shown in Figure 4, is then formulated to minimise the H^∞ norm of the transfer function from $w = \left[\begin{array}{cc} I_n & i_N \end{array}\right]^T$ to $z = \left[\begin{array}{cc} z_1 & z_2 \end{array}\right]^T$, denoted $T_{zw} = \mathcal{F}_l(\tilde{P}, C)$. The closed-loop system can be represented as

$$\begin{array}{c} \left[\begin{array}{c} z \\ y \end{array}\right] = \tilde{P} \left[\begin{array}{c} w \\ u \end{array}\right], \\ u = Cy, \end{array}$$

where $\tilde{P}$ is the generalised plant and C is the controller to be designed.

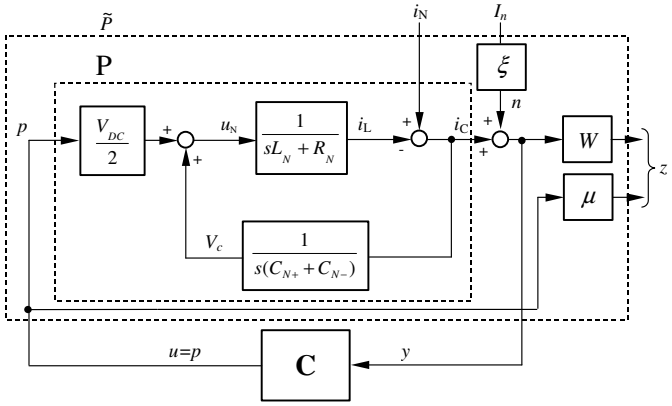

Fig. 4. Formulation of the H^∞control problem for neutral point control

C. Realisation of the Plant P

The inductor current i_L and the voltage V_C are chosen as state variables $x = \left[\begin{array}{cc} i_L & V_c \end{array}\right]^T$. The output signal from the plant P is the capacitor current $i_C = i_N - i_L$, i.e., the difference between the neutral current and the current through the inductor. The plant P can be then described by the state equation

$$\dot{x} = Ax + B_1 i_N + B_2 u \tag{2}$$

and the output equation

$$y = e = C_1 x + D_1 i_N + D_2 u \tag{3}$$

with

$$A = \left[\begin{array}{cc} -\frac{R_N}{L_N} & \frac{1}{L_N} \\ -\frac{1}{C_{N+}+C_{N-}} & 0 \end{array}\right],$$

$$B_1 = \left[\begin{array}{c} 0 \\ \frac{1}{C_{N+}+C_{N-}} \end{array}\right], \quad B_2 = \left[\begin{array}{c} \frac{V_{DC}}{2L_N} \\ 0 \end{array}\right],$$

$$C = \left[\begin{array}{cc} -1 & 0 \end{array}\right], \quad D_1 = \left[\begin{array}{c} 1 \end{array}\right], \quad D_2 = \left[\begin{array}{c} 0 \end{array}\right].$$

The corresponding plant transfer function is then

$$P = \left[\begin{array}{cc} D_1 & D_2 \end{array}\right] + C_1(sI - A)^{-1} \left[\begin{array}{cc} B_1 & B_2 \end{array}\right],$$

or, in short,

$$P = \left[\begin{array}{c|cc} A & B_1 & B_2 \\ \hline C_1 & D_1 & D_2 \end{array}\right]. \tag{4}$$

In the sequel, this notation will be used for transfer functions.

D. Realisation of the generalised plant $\tilde{P}$

Assume that the fundamental frequency of the neutral current is 50Hz, the weighting function W can be realised as a proportional-resonant (PR) filter

$$W = \left[\begin{array}{c|c} A_w & B_w \\ \hline C_w & 0 \end{array}\right], \tag{5}$$

with a high gain at the vicinity of the line frequency while providing smaller gains at all the other frequencies. From Figure 4, the following equations can be obtained:

$$\begin{aligned} y &= i_C + \xi I_n = \xi I_n + \left[\begin{array}{c|cc} A & B_1 & B_2 \\ \hline C & D_1 & D_2 \end{array}\right] \left[\begin{array}{c} i_N \\ u \end{array}\right] \\ &= \left[\begin{array}{c|ccc} A & 0 & B_1 & B_2 \\ \hline C_1 & \xi & D_1 & D_2 \end{array}\right] \left[\begin{array}{c} I_n \\ i_N \\ u \end{array}\right], \end{aligned} \tag{6}$$

$$\begin{aligned} z_1 &= W(i_C + \xi I_n) \\ &= \left[\begin{array}{c|c} A_w & B_w \\ \hline C_w & 0 \end{array}\right] \left[\begin{array}{c|ccc} A & 0 & B_1 & B_2 \\ \hline C_1 & \xi & D_1 & D_2 \end{array}\right] \left[\begin{array}{c} I_n \\ i_N \\ u \end{array}\right] \\ &= \left[\begin{array}{cc|ccc} A & 0 & 0 & B_1 & B_2 \\ B_w C_1 & A_w & B_w \xi & B_w D_1 & B_w D_2 \\ \hline 0 & C_w & 0 & 0 & 0 \end{array}\right] \left[\begin{array}{c} I_n \\ i_N \\ u \end{array}\right] \end{aligned} \tag{7}$$

$$z_2 = \mu u. \tag{8}$$

Combining equations (6), (7) and (8), the realisation of the generalised plant is then obtained as

$$\tilde{P} = \left[\begin{array}{cc|ccc:c} A & 0 & 0 & B_1 & B_2 & \\ B_w C_1 & A_w & B_w \xi & B_w D_1 & B_w D_2 & \\ \hline 0 & C_w & 0 & 0 & 0 & \\ 0 & 0 & 0 & 0 & \mu & \\ \hdashline C & 0 & \xi & D_1 & D_2 & \end{array}\right]. \tag{9}$$

TABLE I

PARAMETERS OF THE NEUTRAL LEG

Parameters	Value	Parameter	Value
L_N	$2.35mH$	C_N	$1000\mu F$
R_N	0.54Ω	f_s	$10kHz$

E. H^∞ Controller Design

The parameters of the neutral leg circuit to be tested are shown in the Table I. The switching frequency is $f_s = 10kHz$. The weighting parameters are chosen to be $\xi = 2.5$ and $\mu = 4$ and the weighting function is chosen as $W(s) = \frac{\omega^2}{s^2+10s+\omega^2}$, with a high gain at $50Hz$ ($\omega = 314rad/sec$).

Using MATLAB $hinfsyn$ algorithm, the H^∞ controller C is obtained as

$$C(s) = \frac{56.0458(s+307)(s^2+258.4s+2.027e005)}{(s+791)(s+250.8)(s^2+10s+9.87e004)}. \quad (10)$$

It can be discretized for implementation. With a sampling frequency of 10kHz, the discretized controller can be obtained using the MATLAB c2d (ZOH) algorithm as

$$C(z) = \frac{0.0054728(z-0.9698)(z^2-1.972z+0.9745)}{(z-0.9239)(z-0.9752)(z^2-1.998z+0.999)}. \quad (11)$$

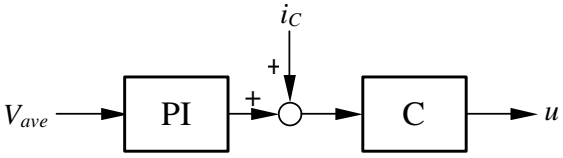

Fig. 5. The proposed cascaded voltage-current controller

IV. Addition of a voltage control loop

As mentioned earlier, the neutral point usually shifts because of capacitors mismatches and/or non-linearity of switches, even if the current i_C is maintained 0. To improve the performance of the proposed strategy there are generally two ways. First is to simply implement offset on the control signal according to the neutral point shift. As a consequence, there is no need to measure voltages across capacitors, and only one sensor to measure capacitor current is necessary for the H^∞ current controller. As the offset is constant, the main drawback of this method is that the neutral point can at some circumstances shifts further. Another way to improve the performance of the proposed strategy is to use an additional voltage control loop. In this case, the capacitors voltages are measured with respect to the neutral point N, as shown in Figure 1(c). The balance between the two capacitor voltages can be achieved by making (1) very small. In this case, the average voltage V_{ave} is used as feedback, which results in a cascaded voltage-current control structure shown in Figure 5. The voltage controller can be chosen as a proportional-integral (PI) controller, which has an infinite DC gain. The H^∞ controller is designed first to meet the specified robustness and error tracking performance and then the voltage controller is fine-tuned with consideration of its influence on the synthesised H^∞ current controller. This control structure brings not only a stable neutral point (current controller), but also a balanced one with respect to the DC-link terminals (voltage control loop).

V. Experimental Validation

The experimental setup consists of an inverter board, a three-phase LC filter, a board consisting of voltage and current sensors, a dSPACE DS1104 R&D controller board with ControlDesk software, and MATLAB Simulink/SimPower software package. The inverter board consists of two independent three-phase inverters and has the capability to generate PWM voltages from a constant $42V$ DC voltage source. The first inverter is used to generate three-phase voltage output and one leg of the second inverter (additional fourth leg) is used to control the neutral point. The parameters of the system are given in Table I.

The proposed controller is compared with a classical controller (voltage and current proportional controllers) proposed in [8] and the H^∞ voltage-current controller proposed in [7]. The control strategies are evaluated under three different situations with $i_N = 0A$, $i_N = 1A$ and $i_N = 2A$. The three-phase inverter is connected to a resistive local load in the open-loop mode to generate the neutral current needed for the tests.

When $i_N = 0A$, Figure 6 (a) shows the currents (i_S, i_R and i_T) of the inverter to generate the neutral current and Figure 6 (b) shows the neutral current i_N, the inductor current i_L and the capacitor current i_C . The neutral point shift, i.e., the average voltage V_{ave}, is shown in Figure 6 (c). The relevant curves are shown in Figure 7 when $i_N = 1A$ and Figure 8 when $i_N = 2A$. The proposed controller maintained a small voltage shift under all three cases. As expected, the majority of the neutral current was forced to flow through the inductor and the current i_C remains nearly 0. The neutral point shift remained almost unchanged when the neutral current was increased. The proposed strategy clearly outperforms the classical and H^∞ voltage-current controllers, with which the neutral point variation and the capacitor current were proportionally increased with the increased neutral current. As a consequence, the neutral point was not well balanced. Moreover, in the case of the classical controller, there is a visible neutral point shift, i.e., an increased DC component in average voltage V_{ave}.

VI. Conclusions

A control strategy is proposed to force the neutral current to flow through the inductor of the neutral leg so that the neutral point is maintained stable and balanced, even for a large neutral current. The experiment results show that, for an increased neutral current i_N, the proposed H^∞ current controller is effective and is able to maintain a stable neutral point. With comparison to the classical and H^∞ voltage-current controllers in literature, the proposed H^∞ current controller demonstrate better performance.

References

[1] H. Nikkhajoei and R. Lasseter, "Distributed generation interface to the CERTS microgrid," *IEEE Transactions on Power Delivery*, vol. 24, no. 3, pp. 1598 –1608, July 2009.

[2] T.-L. Lee and P.-T. Cheng, "Design of a new cooperative harmonic filtering strategy for distributed generation interface converters in an islanding network," *IEEE Transactions on Power Electronics*, vol. 22, no. 5, pp. 1919 –1927, Sept. 2007.

[3] C. Xiarnay, H. Asano, S. Papathanassiou, and G. Strbac, "Policymaking for microgrids," *IEEE Power and Energy Magazine*, vol. 6, no. 3, pp. 66 –77, May-June 2008.

[4] Y. W. Li and C.-N. Kao, "An accurate power control strategy for power-electronics-interfaced distributed generation units operating in a low-voltage multibus microgrid," *IEEE Transactions on Power Electronics*, vol. 24, no. 12, pp. 2977 –2988, Dec. 2009.

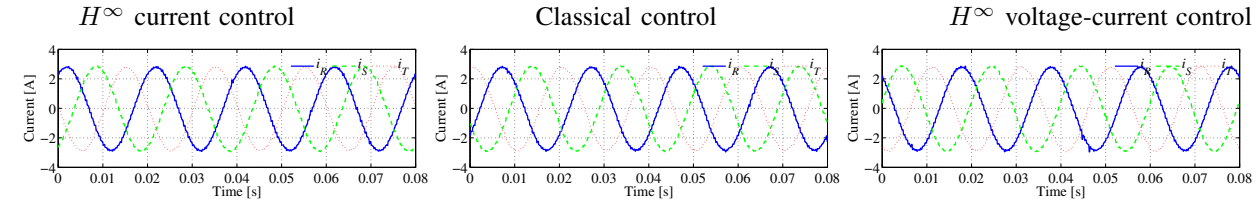

(a) three-phase currents i_R, i_S and i_T of the inverter to generate the neutral current

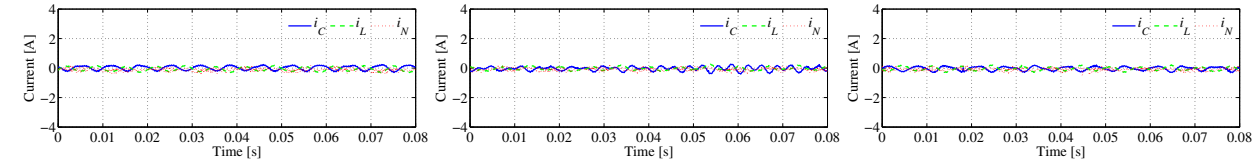

(b) the neutral current i_N, capacitor current i_C and inductor current i_L

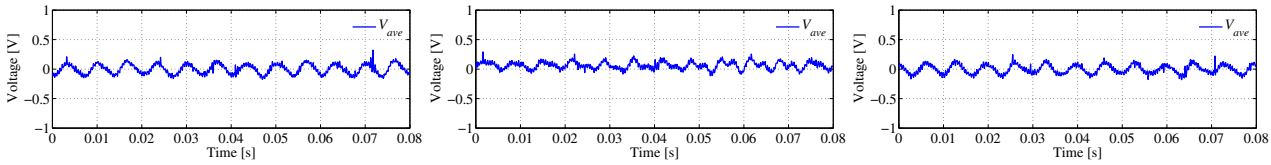

(c) the neutral point shift

Fig. 6. Comparison of neutral point control strategies: $i_N = 0A$

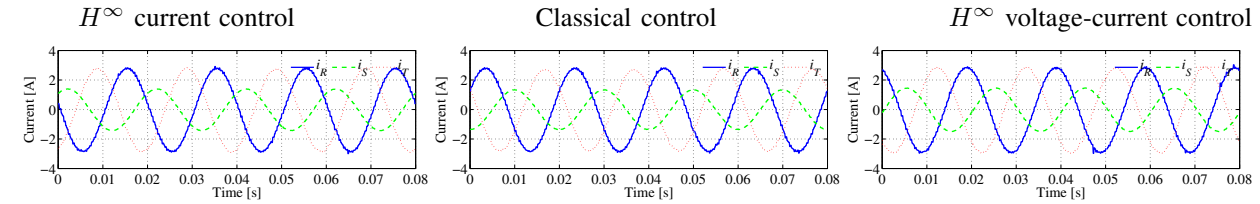

(a) three-phase currents i_R, i_S and i_T of the inverter to generate the neutral current

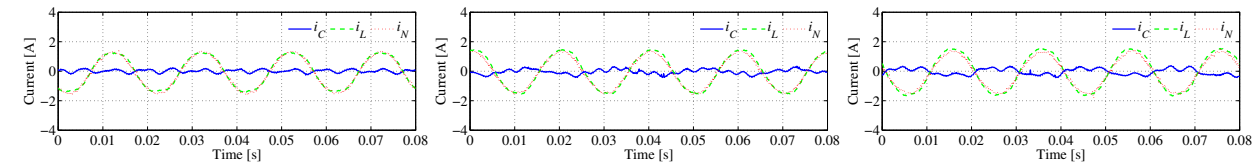

(b) the neutral current i_N, capacitor current i_C and inductor current i_L

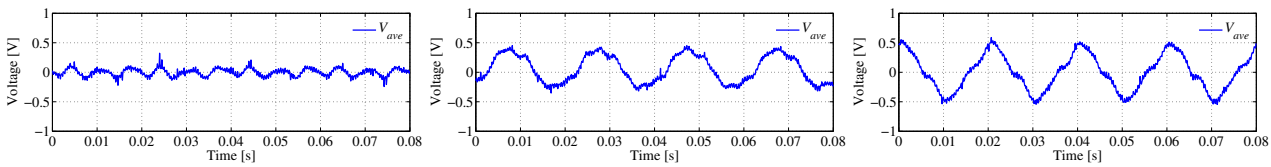

(c) the neutral point shift

Fig. 7. Comparison of neutral point control strategies: $i_N = 1.0A$

[5] C.-L. Chen, Y. Wang, J.-S. Lai, Y.-S. Lee, and D. Martin, "Design of parallel inverters for smooth mode transfer microgrid applications," *IEEE Transactions on Power Electronics*, vol. 25, no. 1, pp. 6 –15, Jan. 2010.

[6] Y. W. Li, D. Vilathgamuwa, and P. C. Loh, "Robust control scheme for a microgrid with PFC capacitor connected," *IEEE Transactions on Industry Applications*, vol. 43, no. 5, pp. 1172 –1182, Sept.-Oct. 2007.

[7] Q.-C. Zhong, J. Liang, G. Weiss, C. Feng, and T. Green, "H^∞ control of the neutral point in four-wire three-phase DC-AC converters," *IEEE Transactions on Industrial Electronics*, vol. 53, no. 5, pp. 1594–1602, 2006.

[8] Q.-C. Zhong, L. Hobson, and M. Jayne, "Classical control of the neutral point in 4-wire 3-phase DC-AC converters," *Electrical Power Quality and Utilisation, Journal*, vol. 11, no. 2, 2005.

[9] J. Salaet, A. Gilabert, J. Bordonau, S. Alepuz, A. Cano, and L. M. Gimeno, "Nonlinear control of neutral point in three-level single-phase converter by means of switching redundant states," *Electronics Letters*, vol. 42, no. 5, pp. 304–306, 2006.

[10] D. Zhou and D. Rouaud, "Experimental comparisons of space vector neutral point balancing strategies for three-level topology," *IEEE Transactions on Power Electronics*, vol. 16, no. 6, pp. 872 –879, Nov. 2001.

[11] A. Bendre, G. Venkataramanan, D. Rosene, and V. Srinivasan, "Modeling and design of a neutral-point voltage regulator for a three-level diode-clamped inverter using multiple-carrier modulation," *IEEE Transactions on Industrial Electronics*, vol. 53, no. 3, pp. 718–726,

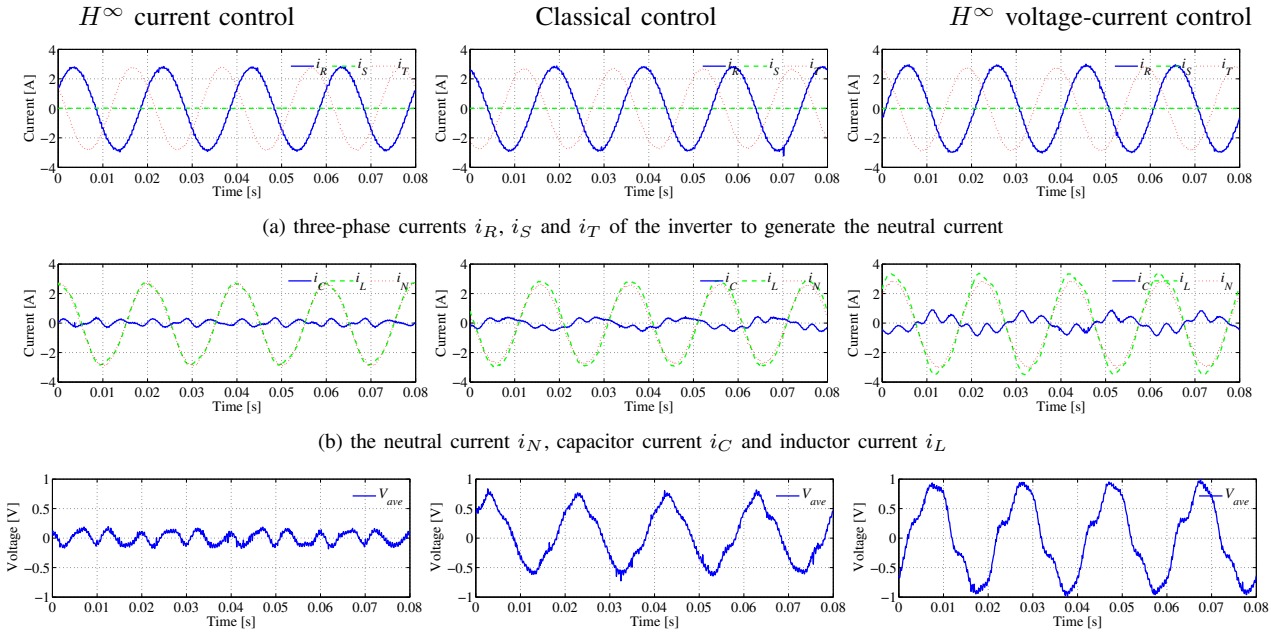

(a) three-phase currents i_R, i_S and i_T of the inverter to generate the neutral current

(b) the neutral current i_N, capacitor current i_C and inductor current i_L

(c) the neutral point shift

Fig. 8. Comparison of neutral point control strategies: $i_N = 2.0A$

2006.

[12] N.-Y. Dai, M.-C. Wong, F. Ng, and Y.-D. Han, "A FPGA-based generalized pulse width modulator for three-leg center-split and four-leg voltage source inverters," *IEEE Transactions on Power Electronics*, vol. 23, no. 3, pp. 1472 –1484, May 2008.

[13] J. Zaragoza, J. Pou, S. Ceballos, E. Robles, C. Jaen, and M. Corbalan, "Voltage-balance compensator for a carrier-based modulation in the neutral-point-clamped converter," *IEEE Transactions on Industrial Electronics*, vol. 56, no. 2, pp. 305 –314, Feb. 2009.

[14] R. Zhang, D. Boroyevich, V. H. Prasad, H. Mao, F. C. Lee, and S. Dubovsky, "Three-phase inverter with a neutral leg with space vector modulation," in *IEEE 12th Applied Power Electronics Conference*, vol. 2, Atlanta, GA, USA, Feb. 1997, pp. 857–863.

[15] J. Liang, T. Green, C. Feng, and G. Weiss, "Increasing voltage utilization in split-link, four-wire inverters," *IEEE Transactions on Power Electronics*, vol. 24, no. 6, pp. 1562 –1569, June 2009.

[16] J. Liang, C. Feng, G. Weiss, and T. Green, "Internal model principle based H^∞ control of a variable neutral-point in an inverter," in *37th IEEE Power Electronics Specialists Conference, PESC '06*, June 2006, pp. 1 – 6.

[17] K. Zhou and J. Doyle, *Essentials of Robust Control*. Upper Saddle River, NJ: Prentice-Hall, 1998.